Journal of Applied Fluid Mechanics, Vol. 18, No. 8, pp. 2043-2052, 2025.
Available online at www.jafmonline.net, ISSN 1735-3572, EISSN 1735-3645.
https://doi.org/10.47176/jafm.18.8.3334

Experimental Study of the Influence of a Blowing Grid on Turbulent Jets Applied to Air Conditioning Systems

A. M. Maiga, A. Khelil†, M. Braikia, M. Khelil, E. Belguebli and A. Fellague Chebra

University of Chlef, Laboratory of Control, Testing, Measurement and Mechanical Simulation, B. P. 151, 2000 Chlef, Algeria

†*Corresponding Author Email:* a.khelil@univ-chlef.dz

ABSTRACT

To overcome the challenges associated with homogenising the aerodynamic parameters of turbulent air jets, special attention must be given to the design of air jet distribution systems. This study aimed to evaluate the performance of two air jet distribution systems, one (AG) equipped with a blowing grid and the other (SG) without, at different frequencies. The frequency parameter was selected due to its proportional relationship with velocity, which allowed for precise control over the inlet flow velocity. Experiments were conducted in a controlled environment using a wind tunnel connected to a test chamber at the Control, Testing, Measurement, and Mechanical Simulation Laboratory of the University of Chlef. The results showed that in the axial direction, the blowing grid caused a reversal in velocity trends, indicating recirculation zones, especially at a frequency N_1=40Hz. Conversely, the gridless configuration exhibited a more uniform velocity distribution. At a frequency N_2=50Hz, the increase in instabilities induced turbulence and flow disturbances, leading to a degradation of the velocity distribution. In the radial direction, the blowing grid improved the diffusion of kinetic energy, resulting in a more homogeneous jet spread and a uniform velocity distribution, especially further from the nozzle. The turbulence intensity in the AG configuration increased by 4% near the chamber wall, a finding that was consistent with shear-induced effects. The system equipped with the blowing grid proved more effective in promoting a consistent radial distribution of airflow. This enhanced flow uniformity is essential for applications requiring precise control of aerodynamic parameters. Ultimately, the blowing grid configuration emerged as the optimal solution for achieving a more homogeneous and stable airflow profile.

Article History

Received December 23, 2024
Revised March 10, 2025
Accepted April 9, 2025
Available online June 3, 2025

Keywords:

Homogenization of environments
Blowing grid
Turbulent air jet
Air conditioning systems
Dynamic fields

1. INTRODUCTION

Air jets resulting from blowers play a crucial role in the field of fluid dynamics. This topic, which has attracted significant attention from researchers in recent decades (Bouhamidi et al., 2020; Chaour et al., 2024), has been the subject of both experimental investigations and numerical simulations of flow phenomena across various application domains, including heat transfer enhancement in industrial environments, aeronautics, electronic component cooling, and others (Mitchell et al., 2016; Bennia et al., 2020; Fellague Chebra et al., 2024). In particular, Zahout et al. (2024) carried out a study of a multi-jet system for thermal comfort applications. Three configurations were analysed: the first had a circular diffuser at the centre, the second had a lobed diffuser, and the third a swirling diffuser. The results indicated that the swirling diffuser configuration was the most efficient, primarily due to its enhanced radial spread. In the field of aeronautics, Hunter et al. (2002) and Shan et al. (2011) studied the exhaust nozzles of gas turbines used in aircraft engines with the aim of increasing engine thrust. The results showed an improvement in engine efficiency while complying with Federal Aviation Administration noise standards. In another study, Lieber and Weir (2007) examined the low-frequency engine noise of a turbofan engine equipped with a nozzle featuring an internal lobed mixer, with a focus on the contributions of combustion noise and exhaust jet noise, using advanced modelling techniques from the NASA Quiet Aircraft Technology program. The study showed that while the mixer reduced the total jet noise, the combustion noise became more significant, especially during flight, and further calibration of the noise prediction models was necessary to accurately predict low-frequency noise. Albayrak et al. (2023) studied the impact of the jet velocity ratio on flow patterns and heat

NOMENCLATURE

A	area of nozzle	Re	Reynolds number
AG	configuration with blowing grid	r	radial co-ordinate
a	length of nozzle	SG	configuration without blowing grid
b	width of nozzle	s	slip of the motor
D	equivalent diameter	U	bulk velocity of configuration with blowing grid for each frequency
N	frequency	u	mean velocity
N_1	40 Hz	U_r	reduced dimensionless velocity
N_2	50 Hz	V	average speed of motor
n	the rotational speed of the motor in revolutions per minute	x	axial co-ordinate
P	number of poles of the motor	ν	kinematic viscosity of the fluid
p	perimeter of nozzle		

transfer in a heated channel, in a context similar to that of electronic components. The study showed that higher jet velocities enhanced heat transfer via convection, thus improving thermal performance. Massip et al. (2012) also conducted an experimental study of turbulent flow around a cube placed at the centre of a channel, which was subjected to both a transverse flow and an impinging jet. The results demonstrated that the effect of the ratio between the Reynolds numbers of the jet and the transverse flow was more pronounced on the flow than the Reynolds number of the transverse flow itself, thus highlighting the importance of vortex and recirculation phenomena in different configurations.

Furthermore, mixing processes are intrinsically linked to turbulence phenomena, and the flow geometry and initial disturbances play a significant role in the generation and transition of turbulence (Dimotakis, 2000; Dia, 2012). An experimental analysis of the axial and radial profiles of temperature and velocity conducted by Braikia et al. (2012) established that the initial geometry of the jet is fundamental in determining its performance and behaviour. It can therefore be concluded that the design of the jet geometry significantly impacts the flow characteristics, with critical implications for various engineering applications. Roux et al. (2009) conducted an experimental study of the dynamics of turbulent round jet impingement at a Reynolds number of 28,000 and an impact distance of five jet diameters. They also explored the influence of geometry. According to Gauntner et al. (1970) and Goldstein & Franchett (1988), the flow field under jet impingement is divided into four distinct regions:

- Region I: This is the fully developed flow region, which stretches from the injection point to the end of the cone orifice's potential core. The flow remains predominantly axial and uniform, exhibiting minimal disturbances or shear effects.
- Region II: This is the established flow zone, where the axial velocity decreases and the jet undergoes further expansion and turbulent development. The jet begins to spread radially, entraining the surrounding fluid.
- Region III: This is the deflection region, where the jet deviates from its initial axial direction due to external forces or surface interactions, resulting in a change in trajectory.

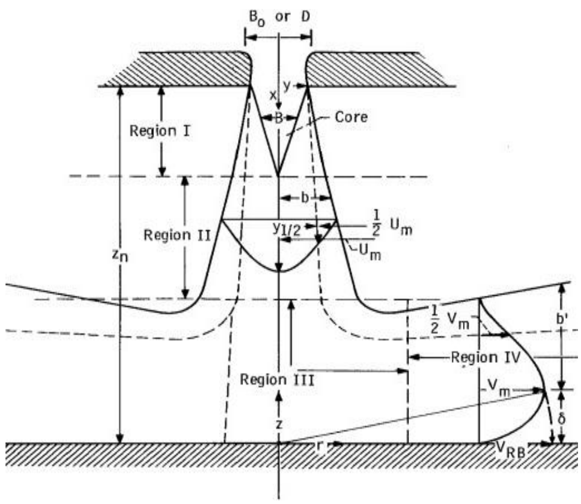

Fig. 1 Diagram of characteristic regions in impinging jet flow (Gauntner et al., 1970)

- Region IV: This is the wall jet region, which is characterised by a predominantly azimuthal velocity profile. The boundary layer thickens radially, and the pressure gradients are virtually zero, indicating a near-inviscid flow near the surface (Fig. 1).

In order to improve the efficiency of air jet diffusion at a lower cost, while enhancing the aesthetic design of air terminal units, a "passive" method is employed (Bennia et al., 2016). This method involves blowing an air jet through a diffuser grid. The presence of a diffuser grid in such installations has proven effective in enhancing heat and mass transfer efficiency, and this passive control mechanism helps to improve the air distribution within the building (Meslem et al., 2012). Anderson and Spall (2001) evaluated the performance of the turbulent RSM model and the standard k-ε model in simulating two turbulent rectangular parallel jets. Numerical predictions were compared with experimental results obtained using a hot-wire anemometer, and excellent agreement was found regarding the merge location and the combined point. Furthermore, the CFD methods employed were able to accurately predict mean velocity profiles in the symmetry plane. The amplitude and decay of the predicted normal stress profiles along the symmetry plane of the flow field were in good agreement with the experimental results, although both turbulence models exhibited a narrower jet envelope width compared to the experimental measurements. In the context of improving air distribution, Aziz et al. (2012) investigated the airflow characteristics of vortex, round, and square diffusers and the impact of these on thermal comfort in a ventilated room. Their study revealed that the velocity decay coefficient was similar for both round and square diffusers, but was 2.6 times higher for the vortex diffuser, reflecting its superior thermal performance. Using a similar optimisation approach, Bragança (2017) designed an innovative air diffuser by integrating lobed inserts into standard commercial diffusers without altering the manufacturing process. Real-world tests demonstrated that these inserts enhanced air mixing, thereby optimising thermal comfort without affecting pressure losses or acoustics, and making this solution viable for buildings.

The primary objective of the present study is to analyse the impact of integrating a diffuser grid on the aerodynamic behaviour of the flow. To achieve this, a detailed evaluation of both axial and radial velocity profiles will be conducted to better understand how the grid influences the flow distribution and its overall efficiency. This analysis will characterise the variations in the fluid velocity as a function of position, and will provide critical insights into the effects of the diffuser grid on the flow dynamics. Particular attention will be paid to the homogeneity of the resulting jet, as this is a key aspect of optimising the performance of air distribution systems.

2. EXPERIMENTAL FACILITY AND MEASUREMENT APPARATUS

The experimental setup was designed to generate a turbulent air jet within a controlled room. The tests were conducted in a test volume of 450 × 400 × 300 mm; these dimensions enabled us to carry out tests under horizontal turbulent jet conditions with unfavourable pressure forces.

The room, which was constructed from Plexiglas, was equipped with several circular openings on its upper surface to allow for the insertion of a velocity sensor. The openings were spaced in both the axial and radial directions at 0.41D, where D represents the equivalent diameter of the cross-section through which the air flow entered the chamber. This interval was selected for technical reasons, as it facilitated the measurement process. Air was blown into the room by a Fansan AKTIF aspirator, the specifications of which are given in Table 1. In addition, a velocity controller, as described in Table 2, was integrated into the system to enable the adjustment of velocity through the proportional relationship between frequency and velocity. This instrument also measures several important parameters, such as current intensity, voltage (both AC and DC), resistance, capacitance, and frequency.

The flow velocity was measured using a hot-wire anemometer (model Velocicalc Plus Air 9565-X Velocity Meter), a high-precision, multifunctional instrument which allows data to be displayed on a screen, printed, or exported to a spreadsheet program, thus facilitating seamless data transfer to a computer for statistical analysis. The velocity accuracy was within ±0.015 m/s (Khelil et al., 2015).

Table 1 Characteristics of the Fansan AKTIF aspirator

Power (P) [W]	250
Voltage (V) [V]	230
Rotational speed (Ω) [RPM]	2800
Frequency (N) [Hz]	50

Table 2 Characteristics of the TMT47503 multimeter

Feature	Range	Accuracy
DC voltage	600 mV / 6 V / 60 V / 600 V / 1000 V	± (0.5% + 3)
AC voltage	6 V / 60 V	± (0.8% + 3)
	600 V / 750 V	± (1.0% + 10)
DC current	60 µA / 60 mA / 600 mA	± (0.8% + 3)
	10 A	± (1.2% + 3)
AC current	60 mA / 600 mA	± (1.0% + 3)
	10 A	± (1.5% + 3)
Resistance	600 Ω / 6 kΩ / 60 kΩ / 600 kΩ / 6 MΩ	± (0.8% + 3)
	60 MΩ	± (1.0% + 30)
Capacitance	10 nF	± (4.0% + 30)
	100 nF / 1000 nF / 10 µF / 100 µF / 1000 µF	± (4.0% + 3)
	10 mF / 100 mF	± (5.0% + 3)
Frequency	10 Hz / 100 Hz / 1000 Hz / 10 kHz / 100 kHz/1000 kHz / 10 MHz	± (1.0% + 3)
Duty cycle	1% ~ 95%	± (2.0% + 3)

To ensure precise calibration of the VelociCalc Plus Air Velocity Meter, it is essential to use a calibrated reference instrument, such as a hot-wire anemometer (VelociCalc Plus Air Velocity Meter). A stable environment was established to ensure that the air velocity remained constant and free from turbulence, thereby eliminating any potential sources of error. The VelociCalc Plus probe was then positioned within the generated airflow, with several measurements taken at different points along the flow. The results obtained in this way were compared with those from the calibrated instrument to confirm the instrument's reliability and accuracy.

The equivalent diameter is given by (Loukarfi, 2021):

$$D = \frac{4A}{p} = \frac{2ab}{(a+b)} \tag{1}$$

where:

A : area of nozzle

p : perimeter of nozzle

a : length of nozzle

b : width of nozzle

After installation of the experimental setup, calibration of the measurement device was conducted to ensure the accuracy and reliability of the collected data.

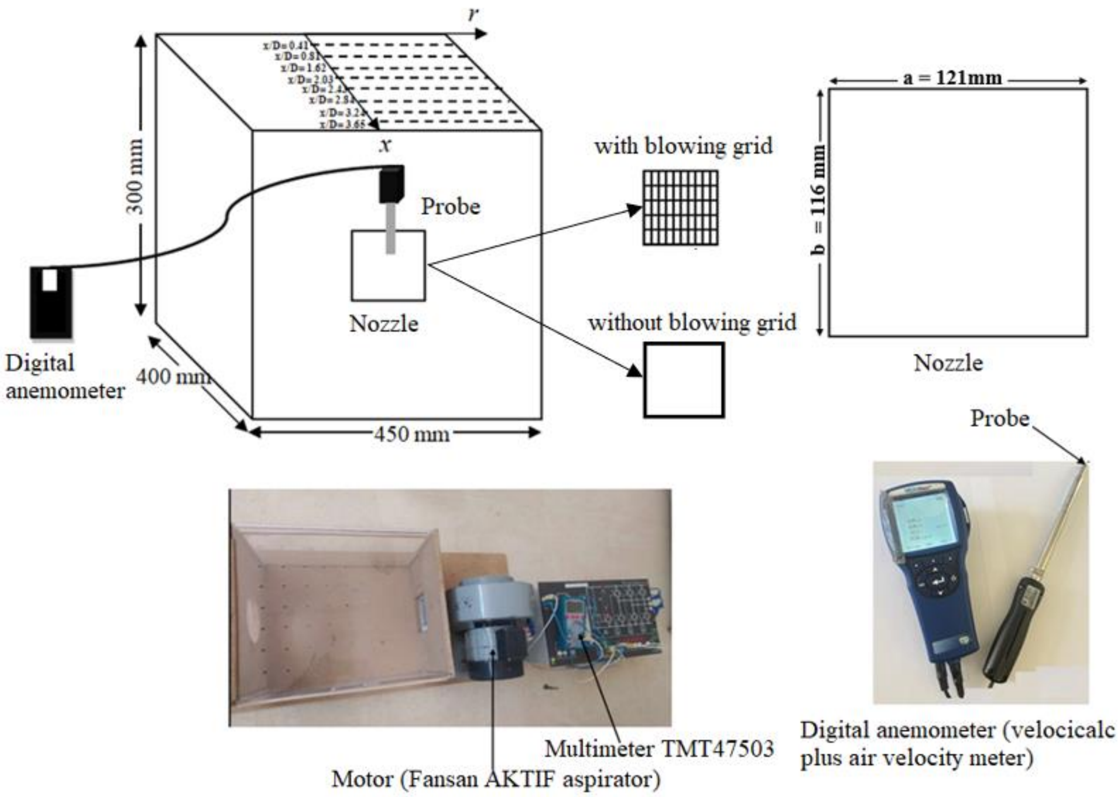

Fig. 2 Experimental setup

Two distinct frequencies were studied: N_1= 40 Hz and N_2= 50 Hz. For each frequency, the velocimeter was inserted into the chamber in two orientations, axial and radial, through the circular openings previously made in the upper surface of the room. At each measurement station, the average flow velocity was determined.

The average speed of a motor is proportional to the frequency, and can be determined as follows (Wildi, 2014):

$$V = \frac{\pi n}{30} \tag{2}$$

where the rotational speed n is given by (Wildi, 2014):

$$n = \frac{60N}{P}(1 - S) \tag{3}$$

and

n is the rotational speed of the motor,

N is the frequency of the alternating current,

P is the number of poles of the motor,

s is the slip of the motor.

3. ESTIMATION OF MEASUREMENT ERROR

The reduced dimensionless velocity (U_r) was obtained with reference to the bulk velocity at the outlet of the blowing orifice U (Bennia et al., 2016) as follows:

$$U_r = \frac{u}{U} \tag{4}$$

$$\frac{\Delta U_r}{U_r} = \frac{\Delta u}{u} + \frac{\Delta U}{U} \tag{5}$$

The uncertainty associated with the velocity measurements was estimated to be less than 4 %.

4. RESULTS AND DISCUSSIONS

4.1 Axial Velocity

The axial velocity distribution, shown in Fig. 3, illustrates the evolution of the velocity profile at different frequencies for the two experimental configurations, with and without the blowing grid.

In the configuration with the blowing grid at frequency N_1=40 Hz (see Fig. 3(a)), the velocity curve follows a Gaussian profile. Initially, the velocity increases gradually as the axial position increases. However, starting at station *x*=2.05D, a reversal of this trend is observed, marking the onset of a deceleration phase. This transition from acceleration to deceleration can be explained by the presence of recirculation zones, which introduce disturbances into the velocity field and directly affect the jet's behaviour. These recirculation zones result from the complex interactions between the jet and the blowing grid, causing a reversal of flow in certain regions. The recirculation zones can be identified by a velocity profile that abruptly changes direction. This change in direction is induced by a low-pressure region.

At frequency N_2 (Fig. 3(b)), the maximum velocity is observed near the nozzle, where the jet exhibits a distinctly high velocity. However, this velocity drops sharply as the

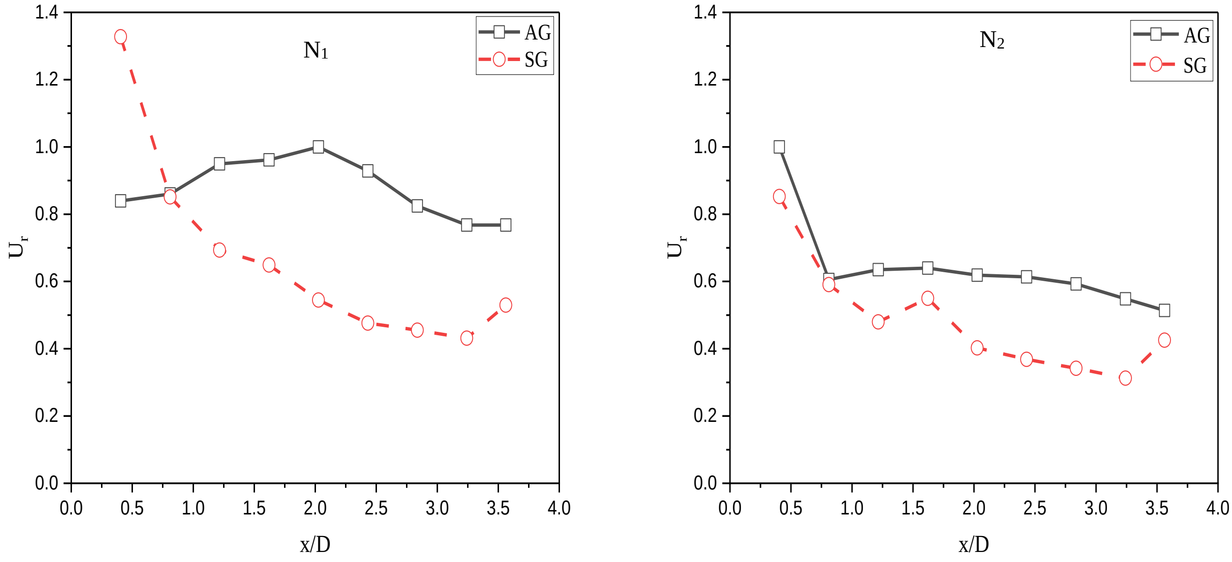

(a) (b)

Fig. 3 Velocity distribution along the axial direction at r=0

distance from the nozzle increases. This rapid decrease is attributed to the attenuation of the jet's dynamic effect in the region near the nozzle (the potential core region). The rapid decline in the potential core region can be explained by the jet expansion, accompanied by a reduction in axial velocity due to the dissipation of kinetic energy through turbulence, as well as the interaction with the ambient fluid. Starting at *x*=0.82D, a slight recovery in velocity is observed, although this increase is weak and gradual. Beyond this station, the velocity undergoes another axial decrease due to the expansion of the jet, indicating that the effect of the blowing grid becomes less significant as the distance from the nozzle increases.

Compared to the configuration with the blowing grid, the axial velocity distribution in the configuration without the grid shows notable variations, both in the velocity distribution and in the grid's effect on the overall flow dynamics.

At frequency N_1, in the configuration without the blowing grid, the axial velocity follows a relatively uniform distribution, with the maximum velocity located near the nozzle. As the axial distance increases, the velocity gradually decreases, but much more slowly than in the configuration with the blowing grid. This rapid decrease in the axial velocity explains the transfer of energy to the radial direction. This behaviour suggests more homogeneous flow diffusion in the configuration without the grid, where the stabilising effect of the grid is less pronounced.

In contrast, at frequency N_2=50 Hz, a recirculation zone forms within the flow, signalling an increase in flow instability. This region, contains turbulence and vortices that disrupt the jet's structure, and which are particularly amplified by the high jet velocity at this frequency. The intense dynamics of the jet, combined with the increased instability in this zone, favour an increased energy transfer between fluid layers, thus intensifying the turbulence. These effects lead to a degradation of the velocity distribution, causing more pronounced flow disturbances in the areas influenced by the recirculation zones.

The increase in instability at frequency N_2 significantly alters the velocity distribution within the flow, particularly in the areas affected by recirculation zones. These instabilities promote mixing and turbulent diffusion, resulting in a more disturbed flow. Consequently, the velocity profile becomes more irregular, and the jet loses coherence, especially in regions where recirculation occurs. The intensified turbulence and energy exchange between fluid layers contribute to the breakdown of the velocity field, making the flow more unpredictable and unstable.

4.2 Radial Velocity

The radial velocity distribution, presented in Fig. 4, shows the evolution of the velocity profile at different frequencies for the two experimental configurations, with and without the blowing grid.

At the lower frequency N_1=40 Hz, both configurations (with and without the blowing grid) exhibit a similar radial velocity distribution near the nozzle, characterised by a reduction in velocity as the distance from the nozzle increases. This velocity decrease can be explained by the interaction between the blown air and the chamber wall. However, notable differences emerge further from the nozzle. At *x*=0.41D, the configuration without the blowing grid shown in Fig. 4(a) has significantly higher velocities, indicating a more concentrated and less disturbed jet. In contrast, at *x*=0.82D (Fig. 4(c)), both configurations follow a similar trend, with an initial increase in velocity followed by a subsequent decrease. However, the configuration without blowing experiences faster velocity attenuation, which can be attributed to the higher dissipation of the jet's kinetic energy. In contrast, the configuration with the blowing grid maintains some flow stability, as the rate of velocity decay is reduced by creating recirculation zones, which help delay the dissipation of kinetic energy.

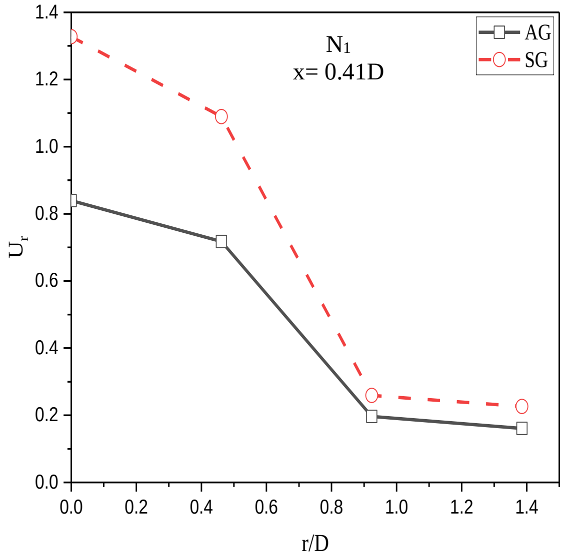
N1
x= 0.41D
AG
SG
Ur
r/D

(a)

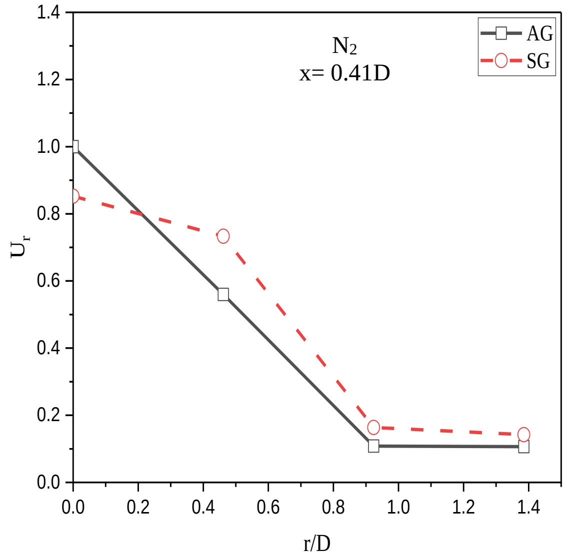
N2
x= 0.41D
AG
SG
Ur
r/D

(b)

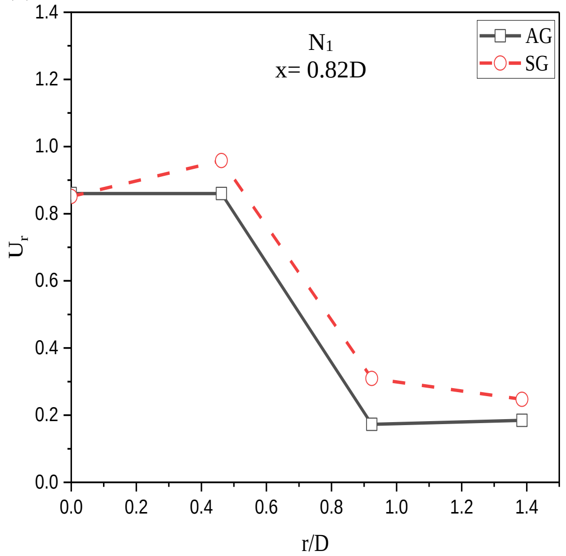
N1
x= 0.82D
AG
SG
Ur
r/D

(c)

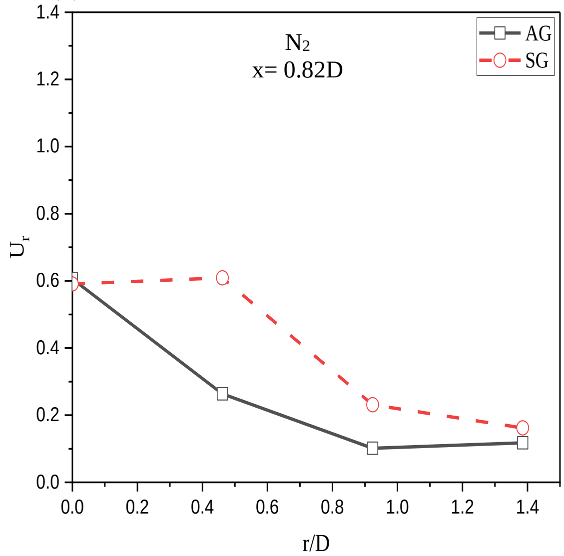
N2
x= 0.82D
AG
SG
Ur
r/D

(d)

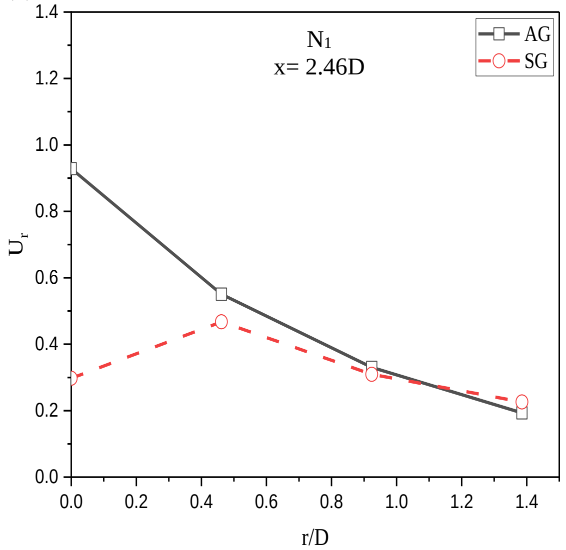
N1
x= 2.46D
AG
SG
Ur
r/D

(e)

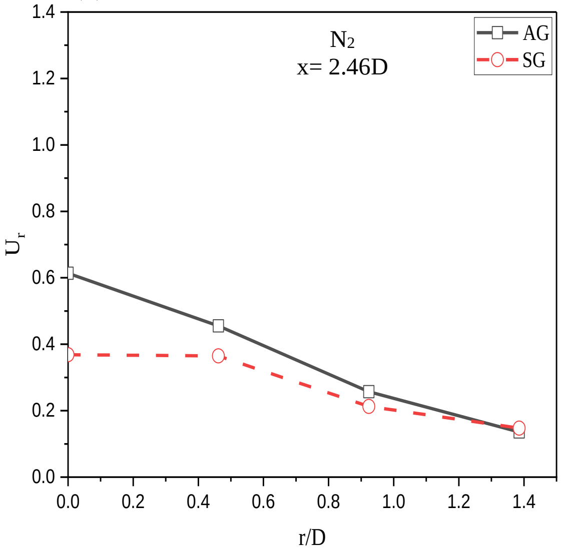
N2
x= 2.46D
AG
SG
Ur
r/D

(f)

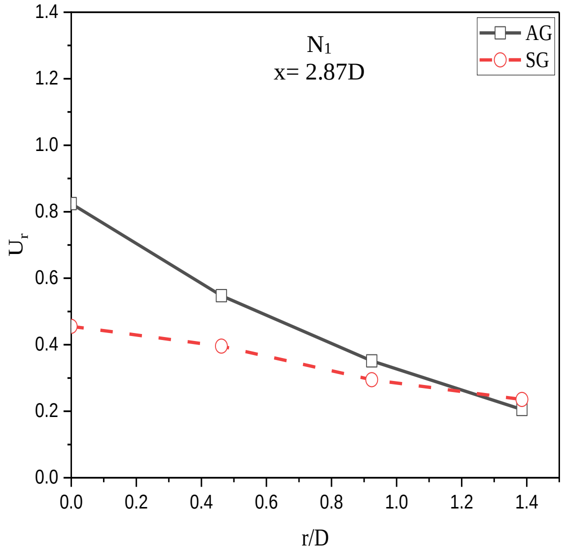

(g)

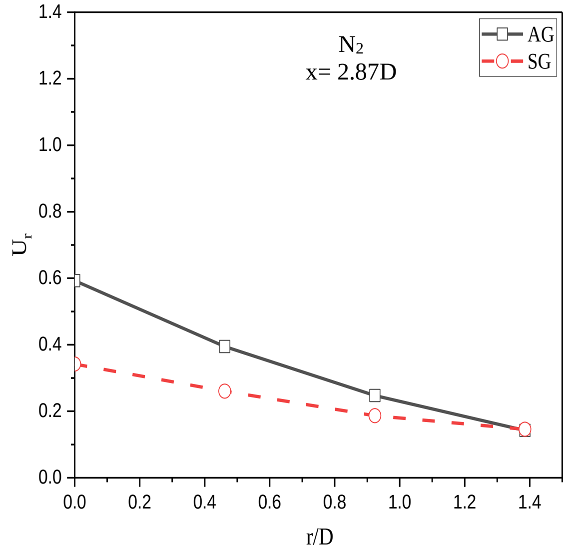

(h)

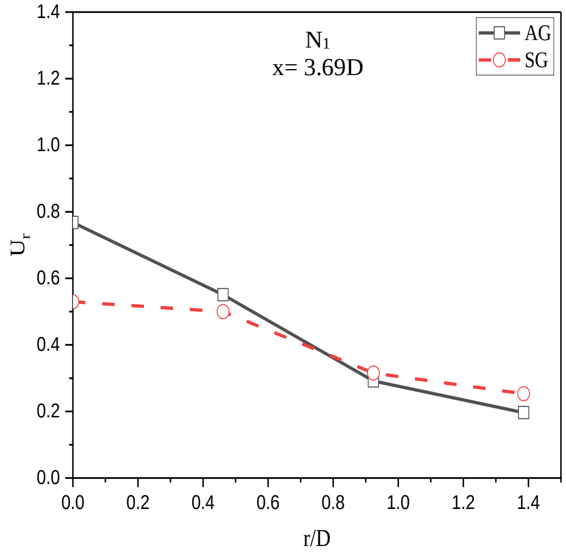

(i)

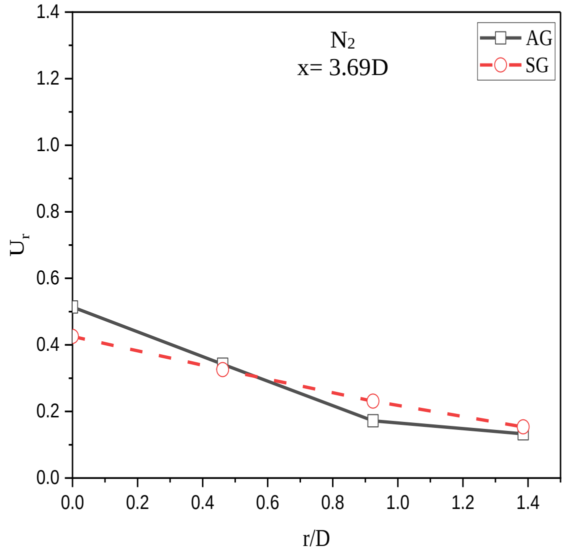

(j)

Fig. 4 Radial velocity distribution

The configuration with the blowing grid at *x*=2.46D, shown in Fig. 4(e), has a higher velocity amplitude compared to the configuration without blowing. This difference is primarily due to the influence of the blowing grid, which promotes better energy dispersion within the flow, allowing the jet to extend further. In contrast, the velocity in the no-blowing grid configuration decreases more sharply due to the turbulence and the recirculation zone that forms.

At *x*=2.87D, the effect of the blowing grid becomes particularly pronounced. At this station, the configuration with the grid shows a significantly higher velocity amplitude, indicating a more extended and better-distributed jet (see Figs. 4(g) and (i)). The presence of the blowing grid not only helps maintain higher kinetic energy within the flow but also optimises the radial velocity distribution, thereby increasing the jet's range. This extended range is a direct result of the blowing grid's modulation of the jet profile, which helps preserve the integrity of the flow over a longer distance, thus reducing energy losses.

At the higher frequency N_2=50 Hz, the configuration with the grid also exhibits higher maximum velocities near the nozzle compared to the no-grid configuration. However, the velocity profiles of both configurations, shown in Figs. 4 (b), (d), and (f), respectively, remain relatively similar. In both cases, the velocity decreases near the nozzle, which is followed by a slight increase and then another decrease further from the nozzle. This behaviour is primarily due to the intense turbulence induced by the interaction between the jet and its surroundings, which leads to the redistribution of energy within the flow in both configurations.

Starting at station *x*=2.87D, the influence of the blowing grid becomes more significant (see Figs. 4(h) and (j)). The recirculation zones present in the no-blowing grid

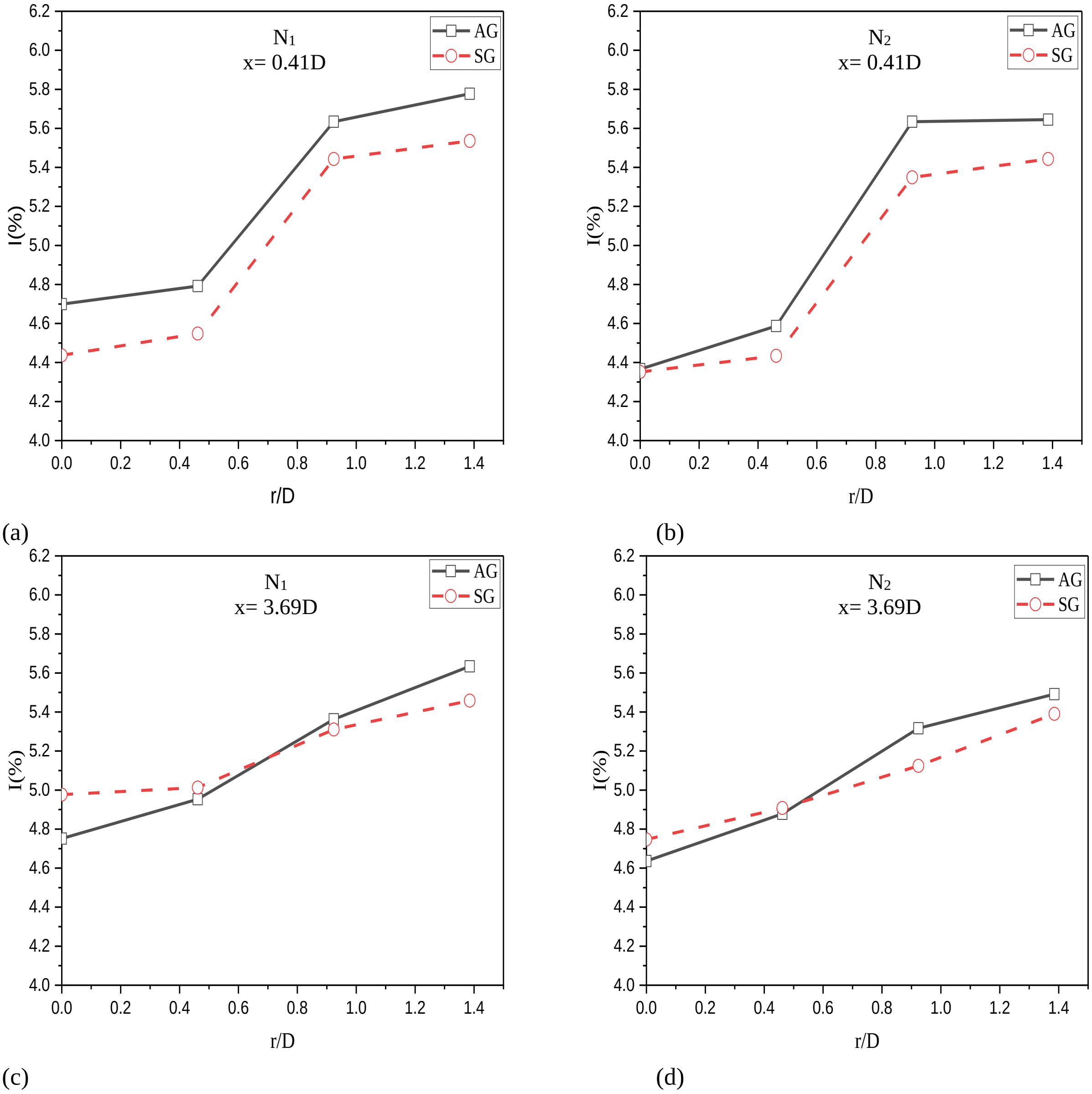

Fig. 5 Turbulence intensity along the radial direction

configuration gradually diminish, leading to a more uniform velocity distribution in the radial direction in the configuration with the blowing grid. This improvement in radial distribution is indicative of flow stabilisation induced by the grid, which allows for more efficient energy management and a better-homogenised velocity field. In the absence of recirculation zones, the configuration with the blowing grid benefits from more consistent velocity diffusion, whereas the no-grid configuration experiences a less uniform distribution and additional flow disturbances due to the recirculations. Thus, the stabilising effect of the blowing grid, especially beyond x=2.87D, significantly enhances both the range and homogeneity of the jet.

4.3 Turbulence Intensity

The turbulence intensity for both configurations at stations x=0.41D and x=3.69D is shown in Fig. 5. It is generally observed that the turbulence intensity increases closer to the chamber wall. This intensification can be explained by dynamic phenomena related to fluid-wall interactions, which are particularly pronounced in air flows. Near the wall, the air experiences significant shear effects, which enhance the turbulence. The velocity gradients, amplified by the boundary layer, promote the formation of complex vortex structures, directly contributing to the rise in turbulence intensity.

Close to the nozzle, the turbulence intensity is significantly higher (see Figs.5(a) and (b)) than farther away from it (see Figs.5(c) and (d)). Further away from the nozzle, the turbulence gradually dissipates due to friction and air diffusion, resulting in a decrease in intensity.

The value of the intensity can be obtained using the following formula (Khelil et al., 2015; Russo & Basse, 2016):

$$I = 0.16(Re)^{-\left(\frac{1}{8}\right)} \tag{6}$$

$$Re = \frac{uD}{\nu} \tag{7}$$

where :

u is the velocity of the fluid,

D is the diameter of the nozzle,

ν is the kinematic viscosity of the fluid.

5. CONCLUSION

This study presents an experimental analysis of an air distribution system for air conditioning applications. The primary objective was to examine the influence of a blowing grid in terms of optimising air distribution. This optimisation was tested using two systems: one equipped with a diffuser grid (AG), and the other without (SG), at frequencies N_1 and N_2, with a margin of error of 4%. The frequency variation highlighted how the air distribution changes between frequencies, with more pronounced recirculation zones occurring when transitioning from one frequency to another.

In the axial direction, the configuration with the blowing grid displayed a reversal in the velocity trend after a certain distance, suggesting the presence of recirculation zones, which were particularly evident at frequency N_1. In contrast, in the gridless configuration, the velocity distribution was more uniform. However, the increase in instabilities, particularly at frequency N_2, induced turbulence and flow disturbances. At this frequency, the recirculation zones exacerbated the degradation of the velocity distribution, thereby contributing to a more disturbed jet dynamics.

In the radial direction, the stabilising effect of the blowing grid became especially evident as the distance from the nozzle increased. Indeed, the grid facilitated better management of kinetic energy diffusion, leading to a more homogeneous jet spread and a more uniform radial velocity distribution, an effect that was not observed in the gridless configuration. Moreover, at frequency N_2, although both configurations exhibited similar velocity profiles, the blowing grid played a key role in mitigating disturbances and maintaining a better air distribution, particularly beyond the station at x=2.87D.

A turbulence intensity analysis also revealed that the presence of the blowing grid increased turbulence by 4% near the chamber wall, a finding that is consistent with the expected effects of shear-induced turbulence. This turbulence was more pronounced near the nozzle but decreased as the distance from the nozzle increased due to the dissipation of turbulent energy.

In view of its advantages in regard to radial propagation as the distance from the nozzle increases, the system with the blowing grid appears better suited to addressing air diffusion issues in larger spaces or environments.

This study has some limitations, particularly in terms of thermal factors, as thermal parameters were not considered. Future studies are strongly recommended to incorporate these parameters. This integration could improve the accuracy of the results and provide a more comprehensive understanding of the system's performance under varying thermal conditions. In addition, further investigation into the impact of thermal variables could lead to more optimised solutions for future applications.

ACKNOWLEDGEMENTS

The support extended by the Head of the Laboratory of Control, Testing, Measurement, and Mechanical Simulation, through the provision of essential laboratory resources, is sincerely acknowledged and appreciated.

CONFLICT OF INTEREST

The authors declare that there are no conflicts of interest regarding the research, authorship, or publication of this article.

AUTHORS CONTRIBUTION

A. M. Maiga, and **A. Khelil:** Conceptualization, Investigation, reviewing, Writing original draft, Editingand Supervision; **M. Braikia**, **M. Khelil**, and **E. Belguebli:** Conceptualization, Analysis, Visualization; **A. Fellague Chebra:** Analysis and Reviewing.

REFERENCES

Albayrak, M., Sarper, B., Saglam, M., & Birinci, S. (2023). The role of jet-to-crossflow velocity ratio on convective heat transfer enhancement in the cooling of discrete heating modules. *Thermal Science and Engineering Progres, 37*, 101549. https://doi.org/10.1016/j.tsep.2022.101549

Anderson, E. A., & Spall, R. E. (2001). Experimental and numerical investigation of two dimensional parallel jets. *Transactions of the ASME*, *123*(2), 401-406. https://doi.org/10.1115/1.1363701

Aziz, M. A., Gad, I. A. M., Mohammed, E. S. F. A., & Mohammed, R. H. (2012). Experimental and numerical study of influence of air ceiling diffusers on room air flow characteristics. *Energy and Buildings*, *55*, 738–746. https://doi.org/10.1016/j.enbuild.2012.09.027

Bennia, A., Fellouah, H., Loukarfi, L., & Naji, H. (2020). Experiments and large-eddy simulations of lobed and swirling turbulent thermal jets for hvac's applications. *Journal of Applied Fluid Mechanics*, *13*(1), 103-117. https://doi.org/10.29252/jafm.13.01.29970

Bennia, A., Loukarfi, L., Khelil, A., Mohamadi, S., Braikia, M., & Naji, H. (2016). Contribution to the experimental and numerical dynamic study of a turbulent jet issued from lobed diffuser. *Journal of Applied Fluid Mechanics*, *9*(6), 2957–2967. https://doi.org/10.29252/jafm.09.06.25953

Bouhamidi, Y., Khelil, A., Hadj Meliani, M., Said, N., & Loukarfi, L. (2020). Numerical investigation of the geometry influence on the aerodynamic fields of the free turbulent jets. *Structural Integrity And Life*, *20*, (3), 219–224.

Bragança, P. (2017). *Ventilation par mélange utilisant des dispositifs de diffusion munis d'inserts lobés : analyse des écoulements moteurs et du confort thermique induit* [PhD thesis, University of Rochelle].

Braikia, M., Loukarfi, L., Khelil, A., & Naji, H. (2012). Improvement of thermal homogenization using multiple swirling jets. *Thermal science, 16* (1), 239-250. https://doi.org/10.2298/TSCI101026131B

Chaour, M., Hamadi, B., Boucherma, D., Boulkroune, S., Achour, T., & Chorfi, S. (2024). Numerical study of the interaction between jets in a reheating furnace. *Studies in Engineering and Exact Sciences, Curitiba, 5*(2), 01-14. https://doi.org10.54021/seesv5n2-587.

Dia, A. (2012). *Simulation de jets d'air lobés pour l'optimisation des Unités Terminales de Diffusion d'Air* [PhD thesis, University of Rochelle].

Dimotakis, P. (2000). The mixing transition in turbulents flows. *Journal of Fluid Mechanics, 409*, 69-98. https://doi.org/10.1017/S0022112099007946

Fellague chebra, A., Khelil, A., Braikia, M., & Bedrouni, M. (2024). Comparative analysis of modified jet diffuser geometry for evaluating the impact of rounded edges and chamfered design on cooling efficiency of electronic components in cross flow and impinging jet. *Journal of Thermal Engineering, 10*(4), 961−977. https://doi.org/10.14744/thermal.0000849

Gauntner, J. W., Livingood, J. N. B., & Hrycak, P. **(**1970). *Survey of literature on flow characteristics of a single turbulent jet impinging on a flat plate.* Technical Report, NASA.

Goldstein, R. J., & Franchett, M. E. (1988). Heat transfer from a flat surface to an oblique impinging jet. *Journal of Heat Transfer, 110*, 84-90. http://dx.doi.org/10.1115/1.3250477.

Hunter, C., Presz, W., & Reynolds, G. (2002). *Thrust augmentation with mixer/ejector systems.* 40th AIAA Aerospace Sciences Meeting & Exhibit, 230.

Khelil, A., Naji, H., Braikia, M., & Loukarfi, L. (2015). Comparative investigation on heated swirling jets using experimental and numerical computations. *Heat Transfer Engineering, 36* (1), 43–57. https://doi.org/10.1080/01457632.2014.906279

Lieber, L. S., & Weir, D. S. (2007). Comparison of measured low-frequency engine noise with combustion and jet noise predictions for a turbofan engine with an internal lobed mixer nozzle. *Turbo Expo: Power for Land, Sea, and Air, 47950*, 1511–1520. https://doi.org/10.1115/GT2007-28027

Loukarfi, L. (2021). *Thermique appliquée, pages bleues*. Algiers. ISBN 978-9947-34-231-2

Massip, Y. Rivas, A., Larraona, G. S., Anton, R., Ramos, J. C., & Moshfegh, B. (2012). Experimental study of the turbulent flow around a single wall-mounted cube exposed to a cross-flow and an impinging jet. *International Journal Heat Fluid Flow, 38*, 50–71. https://doi.org/10.1016/j.ijheatfluidflow.2012.07.004

Meslem, A., Bode, F., Nastase, I., & Martin O. (2012). Optimization of lobed perforated panel diffuser: numerical study of orifice geometry. *Modern Applied Science, 59*, 6-12. http://dx.doi.org/10.5539/mas.v6n12p59

Mitchell, M. G., Smith, L. L., Karagozian, A. R., & Smith, O. I. (2016). Emissions measurements from a lobed fuel injector/burner. *American Institute of Aeronautics and Astronautics.* https://doi.org/10.2514/6.1998-802

Roux, S., Brizzi, L. E., & Dorignac, E. (2009). *Dynamics of a round jet impinging a flat wall constrained by acoustic forcing.* 19th French Congress of Mechanics Marseille. https://hal.science/hal-03390814v1

Russo, F., & Basse, N. T. (2016). Scaling of turbulence intensity for low-speed flow in smooth pipes. *Flow Measurement and Instrumentation, 52*, 101–114. https://doi.org/10.1016/j.flowmeasinst.2016.09.012

Shan, G., Zhang, J., & Huang, G. (2011). Experimental and numerical studies on lobed ejector exhaust system for micro turbojet engine. *Engineering Applications of Computational Fluid Mechanics, 5*(1), 141–148. https://doi.org/10.1080/19942060.2011.11015358

Wildi, T. (2014). *Electrical machines, drives, and power systems* (5th ed.). Pearson.

Zahout, N., Braikia, M., Khelil, A., & Naji, H. (2024). Thermal and dynamic characterization of a multi-jet system with different geometry diffusers. *Journal of Thermal Engineering, 10*(2) 404−429. https://doi.org/10.18186/thermal.1456643.